Cumhuriyet Science Journal

e-ISSN: 2587-246X
ISSN: 2587-2680

Cumhuriyet Sci. J., 42(1) (2021) 22-29
http://dx.doi.org/10.17776/csj.812164

Hydrothermal synthesis and crystal structures of a novel Keggin-type polyoxometalate based on 1,10-phenanthroline

Asuman UÇAR [1,*], ***Mükerrem FINDIK*** [2], ***Nuriye KOÇAK*** [3], ***Alper Tolga ÇOLAK*** [4], ***Onur ŞAHIN*** [5]

[1]*Ağrı İbrahim Çeçen University, Education Faculty, Department of Science Education, Ağrı / TURKEY*

[2]*Necmettin Erbakan University, A.K. Education Faculty, Department of Chemistry Education, Research Laboratory, Konya / TURKEY*

[3]*Necmettin Erbakan University, A.K. Education Faculty, Department of Science Education, Konya / TURKEY*

[4]*Kütahya Dumlupınar University, Faculty of Arts and Science, Department of Chemistry, Kütahya / TURKEY*

[5] *Sinop University, Faculty of Health Sciences, Department of Occupat Health & Safety, Sinop / TURKEY*

Abstract

Herein a novel inorganic-organic hybrid Keggin-type heteropolymolybdate $[Ni_2Na(C_{12}H_8N_2)_4(BMo_{12}O_{40})(H_2O)_2]$ **(1)** has been synthesized under hydrothermal conditions in aqueous solution. The cyrstal structure was fully characterized by powder X-ray diffraction (XRD), elemental analysis, Fourier-tranform infrared spectrum (FT-IR), Thermogravimetric analysis (TGA) and Scanning Electron Microscopy (SEM) analysis. Single crystal X-ray structural analysis demonstrates that the complex consists of a Keggin anion $[BMo_{12}O_{40}]^{5-}$ polyanion, four 1,10-phenanthroline ($C_{12}H_8N_2$) ligands, two Ni(II) ions, two Na(I) ions and two aqua ligands. The experimental powder X-ray diffraction (XRD) result of the crystal is consistent with the calculated data. The SEM image shows that the compound crystals have a cubic structure.

Article info

History:
Received: 18.10.2020
Accepted: 21.01.2021

Keywords:
Polyoxometalates,
Coordination complexes,
Oxoclusters,
Hydrothermal synthesis,
Keggin.

1. Introduction

Polyoxometalates (POMs) are ametal-oxygen cluster compounds consisting of higher oxidation states of oxo-anions of early transition metals (W^{VI}, Mo^{VI}, $V^{V}$and Nb^{VI}) [1-2]. Polyoxometalates are used as inorganic compound because of their various shapes, large size and rich electronic and magnetic properties [3]. The POM has been extensively studied because of the terminal and active bridging oxygen atoms, tunable composition, the high charge density, and diversity of shape and size [4]. Keggin-type POMs can be used as POM-based inorganic–organic hybrid compounds because of their simple synthesis procedure, thermal stability, large electron density and abundant surfaces [5-7]. POMs have been taken part in many fields such as sensitive devices, medicine, catalysis, nanotechnology, energy storage, photochemistry, materials science, nuclear waste treatment and magnetism due to their excellent topological and electronic versatility [8-18]. In previous studies, polyoxomolybdates have been synthesized such as $[XMo_{12}O_{40}]^{n-}$ (X = As, P, Si, Ge, Ni, Co) [19-22]. The $[BMo_{12}O_{40}]^{5-}$ framework, which is a boron-containing Keggin type polyoxomolybdate anion, was synthesized for the first time by our research group [23]. POMs are widely used as a catalysts for water oxidation [24] and transformation of CO_2 into desirable chemical products [25]. Alamdari et al. synthesized Mo132-MimAM for the oxidation of sulfides and Hasannia et al. synthesized LDH-PWFe for the oxidation of alcohols [26-27]. These studies by researchers have shown that POMs have great potential in catalysis studies and paved the way for new studies. In the present study, a new organic-inorganic hybrid based on 1,10-phenanthroline($C_{12}H_8N_2$) ligands and Keggin anion $[BMo_{12}O_{40}]^{5-}$ was synthesized to support new catalysis studies, which is the main purpose of our study. It is also thought that the POM synthesized by our group will serve as a new model for the design of transition metal-substituted POM architectures. Because of the high catalytic properties of hybrid POMs, it offers a great variety of catalytic applications with different fields of study, such as redox reactions,

*Corresponding author. *e-mail address: asucar340@gmail.com*

energy, enviromental, biomedical and green chemistry. Herein, the cyrstal $[Ni_2Na(C_{12}H_8N_2)_4(BMo_{12}O_{40})(H_2O)_2]$ (1) was hydrothermally synthesized for the first time and characterized in detail using single crystal X-ray structural analysis, XRD, elemental analysis, FT-IR, TGA and SEM techniques both structurally and morphologically.

2. Materials and Methods

2.1. Reagents and apparatus

All reagents were obtained from commercial resources and used without further purification. Nickel(II)chloride hexahydrate ($NiCl_2.6H_2O$) and hydrochloric acid (HCl) were supplied by Merck. Sodium tungstate dehydrate ($Na_2MoO_4.2H_2O$), boric acid (H_3BO_3) and 1,10-phenanthroline were supplied by Sigma-Aldrich. Perkin-Elmer 2400 CHN (PerkinElmer Inc, USA) elemental analyzer was used for elemental analysis (C, N and H) of sample. The FT-IR spectrum was recorded at room temperature on a Perkin Elmer model 100 ATR-FTIR spectrometer (PerkinElmer Inc, USA). Thermogravimetric analysis (TGA) was carried out with a Setaram thermal gravimetric analyzer (Simultaneous Thermal Analysis, Setaram Instrumentation, France) at a heating rate of 1 °C/min under N_2 atmosphere (25–1000 °C). SEM image was investigated on a Hitachi – SU 1510 at accelerating voltage of 20 kV and magnification of 10.00 kX. Powder XRD measurements were taken using Bruker D.8 Advance (Germany) X-ray diffractometer.

2.2. Preparation of $[Ni_2Na(C_{12}H_8N_2)_4(BMo_{12}O_{40})(H_2O)_2]$ (1)

The compound as synthesized according to our previous article [25].

A mixture of H_3BO_3 (0.186 g, 3.0 mmol), $Na_2MoO_4.2H_2O$ (1.46 g, 6.00 mmol), $NiCl_2.2H_2O$ (0.392 g, 1.65 mmol), 1,10-phenanthroline (0.3 g, 1.5 mmol) and H_2O (20 ml) was stirred for an hour. The pH of the mixture was adjusted to 2 with 6 M HCl. The mixture was allowed to react in a Teflon-lined stainless steel reactor for 7 days at 185 °C. After 7 days of reaction, the product was cooled down to room temperature by 10 degrees per hour and green crystals were obtained (yield 83 %) (Figure 1).

Anal. Calcd. For $C_{48}H_{36}BMo_{12}N_8NaNi_2O_{42}$ (2699.35g/mol): C, 21.34%; H, 1.33%; N, 4.15%. Found: C, 21.52%; H, 1.46%; N, 4.33%. FT-IR (cm^{-1}): 3578, 3062, 1628, 1517, 1429, 1037, 984, 940, 896.

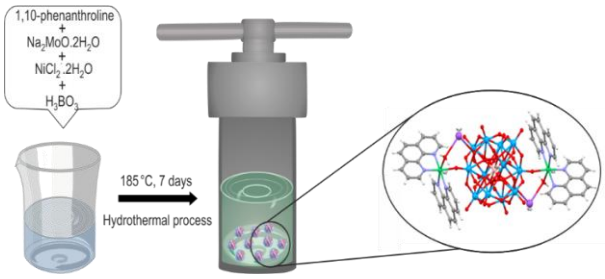

Figure 1. Synthetic routes for the compound.

2.3. X-Ray diffraction analysis

The hydrogen atoms bound to carbon atoms were treated as riding atoms with distances of 0.93 Å. Other H atoms were refined freely. In order to avoid ADP and NPD problems, the EADP command was used to refine the non-H atoms. With SHELXS-2013 [28], the structure of compound **1** was solved by direct methods and refined using full-matrix least-squares methods with SHELXL-2013 program [29] within WinGX [30]. The structural data of compound **1** was collected on Bruker APEX2 (APEX2, Bruker AXS Inc. Madison Wisconsin USA 2013). MERCURY program was used for molecular graphics. Details of data collection and crystal structure determinations are shown in Table 1. Crystallographic data of the structure has been deposited in the Cambridge Crystallographic Data Center with CCDC number 1844844.

3. Results and Discussion

3.1. Structural analysis

The molecular structure unit of compound **1** with the atom labeling is shown in Figure 2. The unsymmetrical unit of compound **1** has been proved to consist of one Na(I) ion, one Ni(II) ion, a half of $[BMo_{12}O_{40}]^{5-}$ polyanion, two phenanthroline ligands and one aqua ligand. The B1 atom is located on the inversion center (1/2, 1/2, 1/2). The polyanion $[BMo_{12}O_{40}]^{5-}$ anion with a Keggin-type structure has a structure with a central BO_4 [B-O bond distances range of 1.60(2)-1.62(3) Å] surrounded by the $Mo_{12}O_{36}$ group with tetrahedron coordination geometry. The oxygen atoms of BO_4 group are disordered over two positions. According to different coordination environments, the Mo–O bonds can be categorized into three groups: Mo-O (terminal oxygen atom) with lengths range between 1.652(11)-1.683(11) Å, Mo-O (bridging oxygen atoms) with lengths range between 1.788(16)-2.039(17) Å and Mo–O (central oxygen atom) with lengths range between 2.34(3)-2.449(19) Å. The Ni(II) ion is coordinated by four nitrogen atoms [Ni-N lengths range between 2.064(13)-2.093(13) Å] from

phenanthroline ligands, one oxygen atom [Ni1-O21=2.115(11) Å] from $[BMo_{12}O_{40}]^{5-}$polyanion and one oxygen atom [Ni1-O23=2.068(12) Å] from aqua ligand, thence indicating a distorted octahedral geometry. At the same time, the Ni1 atom and $[BMo_{12}O_{40}]^{5-}$ polyanion are bridged by Na1 atom, thus produce $[Ni_2Na(C_{12}H_8N_2)_4(BMo_{12}O_{40})(H_2O)_2]$ cluster. Selected bond lengths for NiBWO (Å) are shown in Table 2. The $[Ni_2Na(C_{12}H_8N_2)_4(BMo_{12}O_{40})(H_2O)_2]$ clusters are combined by O-H···O hydrogen bonds, creating 1D supramolecular network running parallel to the [001] direction (Figure 3). Similarly, adjacent $[Ni_2Na(C_{12}H_8N_2)_4(BMo_{12}O_{40})(H_2O)_2]$ clusters are combined by C-H···O hydrogen bonds, generating 1D supramolecular network running parallel to the [010] direction (Figure 4). The combination of O-H···O and C-H···O hydrogen bonds (Table 3) is generating 2D supramolecular network.

The most important step of the experimental studies using UV–Vis spectrophotometry is the selection of the measurement wavelength. Because all the experimental measurements were performed at the selected wavelength. If the correct wavelength is not selected, all experimental results are affected.

Table 1. Crystal data and structure refinement parameters for compound 1

Empirical formula	$C_{48}H_{36}BMo_{12}N_8NaNi_2O_{42}$
Formula weight	2699.35
Crystal system	Triclinic
Space group	P-1
a (Å)	10.789 (3)
b (Å)	13.295 (4)
c (Å)	13.622 (3)
α (°)	69.268 (7)
β (°)	71.433 (6)
γ (°)	77.446 (7)
V (Å^3)	1720.3 (7)
Z	1
Diffractometer	BRUKER D8-QUEST
Temperature (K)	296
F(000)	1292
θ range (º)	3.2-28.4
Measured refls.	77058
Independent refls.	6739
Parameters	454
R_{int}	0.030
S	1.08
R1/wR2	0.113/0.225

Table 2. Selected bond distances for compound 1 (Å)

B1-O1	1.60(2)	B1-O2	1.62(3)	B1-O3	1.61(3)
B1-O4	1.60(3)	Mo1-O21	1.683(11)	Mo1-O9	1.798(17)
Mo1-O18^i	1.841(16)	Mo1-O8	1.982(16)	Mo1-O15^i	2.001(16)
Mo1-O2	2.34(3)	Mo1-O1	2.382(19)	Mo2-O20	1.661(12)
Mo2-O8	1.809(17)	Mo2-O19	1.825(16)	Mo2-O7	1.989(17)
Mo2-O10	2.003(16)	Mo2-O2	2.43(3)	Mo2-O3	2.43(3)
Mo3-O17	1.663(12)	Mo3-O7	1.799(16)	Mo3-O6	1.799(16)
Mo3-O18	2.009(16)	Mo3-O13^i	2.010(16)	Mo3-O3	2.38(3)
Mo3-O1^i	2.407(19)	Mo4-O16	1.658(12)	Mo4-O5	1.788(16)
Mo4-O15	1.805(16)	Mo4-O6	1.996(16)	Mo4-O12	2.023(16)
Mo4-O4^i	2.41(3)	Mo4-O1^i	2.449(19)	Mo5-O14	1.658(11)
Mo5-O13	1.813(17)	Mo5-O11	1.815(16)	Mo5-O19^i	1.991(16)
Mo5-O5	1.992(17)	Mo5-O3^i	2.38(3)	Mo5-O4^i	2.40(3)
Mo6-O22	1.652(11)	Mo6-O12	1.794(16)	Mo6-O10	1.810(16)
Mo6-O11	1.986(16)	Mo6-O9	2.039(17)	Mo6-O4^i	2.41(3)
Mo6-O2	2.43(3)	N1-Ni1	2.084(13)	N2-Ni1	2.093(13)
N3-Ni1	2.064(13)	N4-Ni1	2.074(13)	Ni1-O23	2.068(12)
Ni1-O21	2.115(11)	Na1-O23	2.74(2)	Na1-O18^i	2.98(2)

Symmetry code: (i) −x+1, −y+1, −z+1.

Table 3. Hydrogen-bond parameters for compound 1 (Å, º)

D-H· · ·A	D-H	H···A	D···A	D-H···A
C9—H9···O8^{iii}	0.93	2.60	3.49 (2)	162
C13—H13···O14^{iv}	0.93	2.48	3.14 (2)	128
O23—H23A···O22^{iv}	0.83 (2)	2.36 (6)	2.877 (16)	121
O23—H23B···N1	0.83 (2)	2.58 (8)	3.010 (18)	114

Symmetry codes: (iii) −x+1, −y+2, −z+1; (iv) −x+1, −y+1, −z+2.

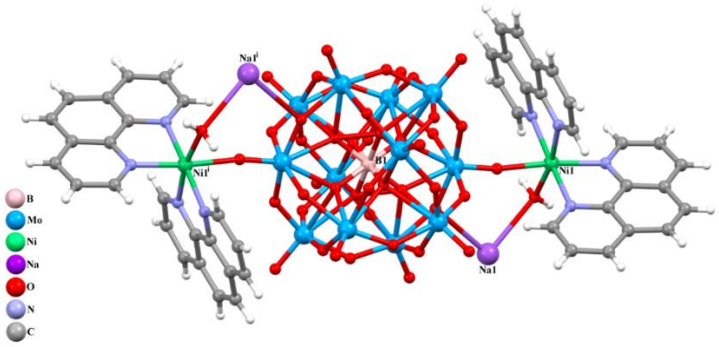

Figure 2. The molecular view of the compound indicating the atom numbering scheme.

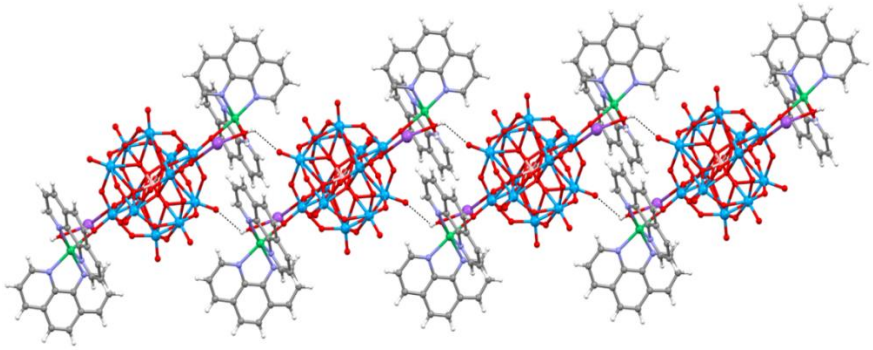

Figure 3. The molecular view of the compound, demostrating the formation of a chain through [001] created by O-H···O hydrogen bonds.

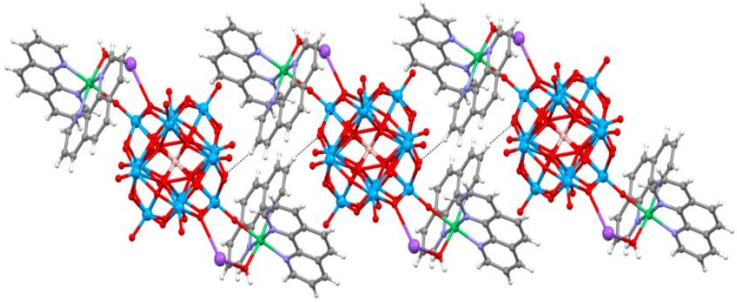

Figure 4. The molecular view of the compound, demostrating the formation of a chain through [010] created by C-H···O hydrogen bond.

3.2. X-ray diffraction

The calculated pattern from single-crystal structures and experimental XRD patterns of the compound is shown in Figure 5. The experimental data is consistent with the calculated patterns, indicating the phase purity of the compound. The preferred orientation of the powder sample may cause differences in intensity. Powder X-ray diffraction results of the structure are similar to other related studies [16,31].

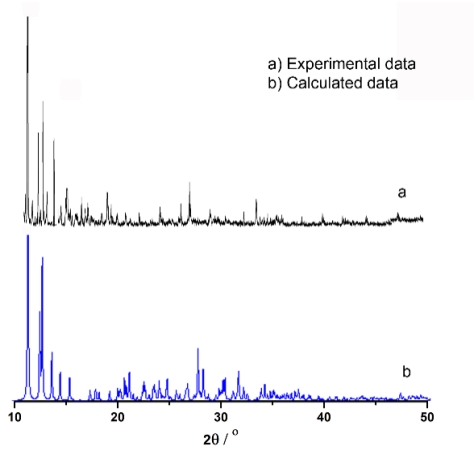

Figure 5. XRD spectra of the compound 1.

3.3. FT-IR spectrum

The crystal contains the identical Keggin POM $[BMo_{12}O_{40}]^{5-}$ and as can seen in Figure 6, the FT-IR spectrum shows the specific vibrations of Keggin type POMs [32]. Characteristics bands of the Keggin unit appeared at 1037, 984, 940 and 896 cm^{-1} can be respectively assigned to B–O, terminal Mo–O, inter-octahedral Mo–O–Mo, and intra-octahedral Mo–O–Mo vibrations [6,33,34]. The band seen at 3578 cm^{-1} can be attributed to the coordinated water [35]. The absorption bands at 3062, 1628, 1517 and 1429 cm^{-1} are assigned to aromatic υ(C-H), azomethine υ(C=N), υ(C=C) and υ(C-N) stretching, respectively [36-39].

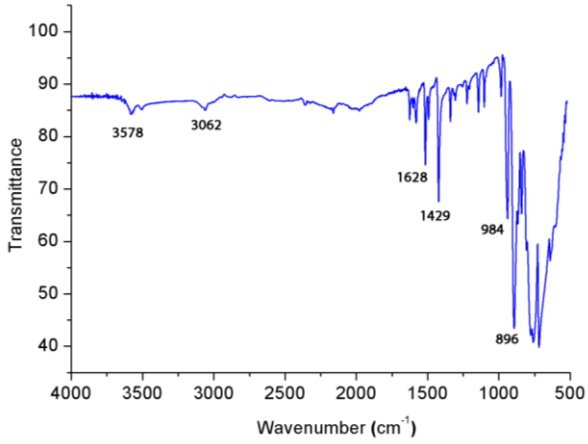

Figure 6. FT-IR spectrum of the compound 1.

3.4. Thermogravimetric analysis

The thermal behaviors of the cyrstal were investigated with the thermal analysis methods. As shown in Figure 7, the water removal causes the slight weight loss below 478 °C [40]. The weight loss in the range of 478-690 °C is attributed to the decomposition of the two 1,10-phenanthroline ligands (calc. 26.7%; found 27.1%) [41].

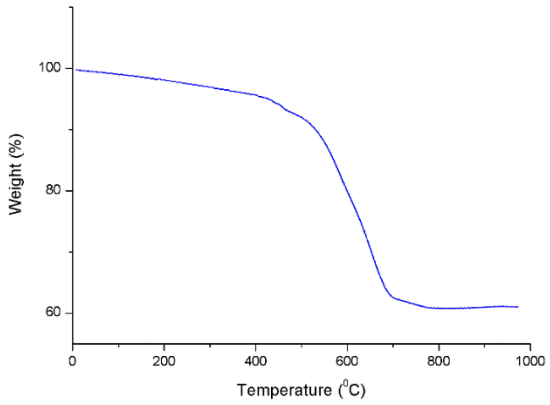

Figure 7. TG curve of the crystal

3.5. SEM analysis

SEM is used to examine the three important factors surfactant morphology (surface structural properties based on shape and size), surface crystallography (ie, surface formation of atoms) and surface composition (in terms of surface composition, compounds and elements). So, the surface property of the compound 1 was checked by using SEM (Figure 8). According to the SEM image, each crystal has a cubic structure.

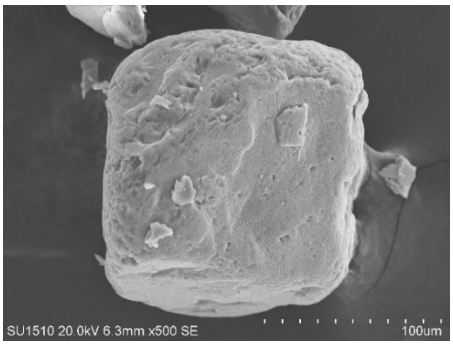

Figure 8. The SEM images of the compound 1.

4. Conclusion

In summary, we have prepared a novel Keggin-type inorganic-organic hybrid compound by using metal Ni(II) ion and 1,10-phenanthroline ($C_{12}H_8N_2$) ligand based on boron atom as the central atom. TGA, FT-IR and XRD methods were used for the structure analysis

of the compound. These analyzes support the results from the single crystal X-ray structural analysis. The content of the structure is determined as a half of $[BMo_{12}O_{40}]^{5-}$ polyanion, two phenanthroline ligands and one aqua ligand according to by single crystal X-ray diffraction. It is thought that a new POM synthesis with the simple synthesis process used in this study will contribute to the development of new inorganic-organic POM materials.

Acknowledgment

This study was supported by the Necmettin Erbakan University Research Foundation (151210002) and for the use of the Bruker D8 QUEST diffractometer, the authors are grateful to Scientific and Technological Research Application and Research Center, Sinop University, Turkey.

Conflicts of interest

The outhors state that there is no conflict of interests.

References

[1] Gupta R., Parbhakar S., Khan I., Behera J.N., Hussain F., Early lanthanoid substituted organic-inorganic hybrids of silico- and germano-tungstates: Syntheses, crystal structures and solid-state properties, *Indian Journal of Chemistry,* 57A (2018) 52-58.

[2] Rezvani M.A., Khandan S., Synthesis and characterization of new sandwich-type polyoxometalate/nanoceramic anocomposite, $Fe_2W_{18}Fe_4$@$FeTiO_3$, as a highly efficient heterogeneous nanocatalyst for desulfurization of fuel, *Solid State Sciences*, 98 (2019) 106036-106044.

[3] Han Z.G., Li S., Wu J.J., Zhai X.L., Hydrothermal synthesis and structural characterization of two new polytungstate-based hybrids, *Journal of Coordination Chemistry,* 64 (2011) 1525–1532.

[4] Mirzaei M., Eshtiagh-Hosseini H., Hassanpoor A., Different behavior of PDA as a preorganized ligand versus PCA ligand in constructing two inorganic-organic hybrid materials based on Keggin-type polyoxometalate, *Inorganica Chimica Acta.*, 484 (2019) 332–337.

[5] Yang D.D., Mu B., Lv L., Huang R.D., The assembly of POM-induced inorganic–organic hybrids based on copper ion sand mixed ligands, *Journal of Coordination Chemistry,* 68 (2015) 752–765.

[6] Arichi J., Pereira M.M., Esteves P.M., Louis B., Synthesis of Keggin-type polyoxometalate crystals, *Solid State Sciences,* 12 (2010) 1866–1869.

[7] Lü Y., Xiao N., Hao X.R., Cui X.B., Xu J.Q., A series of organic–inorganic hybrid compounds formed by $[P_2W_{18}O_{62}]^{6-}$ and several types of transition metal complexes, *Dalton Transactions,* 46 (2017) 14393-14405.

[8] Wang X., Li T., Tian A., Xu N., Zhang R., Introduction of secondary pyridyl-1H-tetrazole derivatives into Keggin–Ag–(1,10-phenanthroline) system for tuning dimensionalities and architectures: assembly and properties, *Journal of Coordination Chemistry,* 69 (2016) 2532–2544.

[9] Dianat S., Bordbar A.K., Tangestaninejad S., Zarkesh-Esfahani S.H., Habibi P., Kajani A.A., ctDNA interaction of Co-containing Keggin polyoxomolybdate and in vitro antitumor activity of free and its nano-encapsulated derivatives, *Journal of The Iranian Chemical Society,*13 (2016) 1895-1904.

[10] Ucar A., Findik M., Gubbuk I.H., Kocak N., Bingol H., Catalytic degradation of organic dye using reduced grapheneoxide–polyoxometalate nanocomposite, *Materials Chemistry and Physics*, 196 (2017) 21-28.

[11] Bicho R.C., Soares A.M.V.M., Nogueira H.I.S., Amorim M.J.B., Effects of europium polyoxometalate encapsulated in silica nanoparticles (nanocarriers) in soil invertebrates, *Journal of Nanoparticle Research*, 18 (2016) 360-366.

[12] Xia S.L.F., Li X., Cheng F., Sun C., Liu J.J., Guo H., An inorganic–organic hybrid supramolecular framework as a high-performance anode for lithium-ion batterie, *Dalton Transactions,* 47 (2018) 5166-5170.

[13] Ishizuka T., Ohkawa S., Ochiai H., Hashimoto M., Ohkubo K., Kotani H., Sadakane M., Fukuzumi S., Kojima T., A supramolecular photocatalyst composed of a polyoxometalate and a photosensitizing water-soluble porphyrindiacid for the oxidation of organic substrates in wate, *Green Chemistry,* 20 (2018) 1975-1980.

[14] Zhao P., Zhang Y., Li D., Cui H., Zhang L., Mesoporous polyoxometalate-based ionic hybrid as a highly effective heterogeneous catalyst for direct hydroxylation of benzene tophenol, *Chinese Journal of Catalysis,* 39 (2018) 334-341.

[15] Dubal D.P., Chodankar N.R., Vinu A., Kim D.H., Gomez-Romero P., Asymmetric Supercapacitors Based on Reduced Graphene Oxide with Different Polyoxometalates as Positive and Negative Electrodes, *Chemsuschem,* 10 (2017) 2742-2750.

[16] Zhang T.T., Hu Y.Y., Zhang X., Cui X.B., New compounds of polyoxometalates and cadmium mixed-organic-ligand complexes, *Journal of Solid State Chemistry,* 283 (2020) 121168-121177.

[17] Wang J., Niu Y., Zhang M., Ma P., Zhang C., Niu J., Wang J., Organo phosphonate-Functionalized Lanthano polyoxomolybdate: Synthesis, Characterization, Magnetism, Luminescence, and Catalysis of H_2O_2-Based Thioether Oxidation, *Inorganic Chemistry,* 57 (2018) 1796-1805.

[18] Rafieea E., Pami N., Zinatizadeh A.A., Eavani S., A new polyoxometalate-TiO_2 nanocomposite for efficient visible photodegradation of dye from waste water, liquorice and yeast extract: Photoelectrochemical, electrochemical and physical investigations, *Journal of Photochemistry & Photobiology A: Chemistry,* 386 (2020) 112145-112156.

[19] An D., Chen Z., Zheng J. Chen S., Wang L. and Su W., Polyoxomatelate functionalized tris(2,2-bipyridyl)dichlororuthenium(II) as the probe for electrochemiluminescence sensing of histamine, *Food Chemistry,* 194 (2016) 966–971.

[20] Yu X.Y., Cui X.B., Lu J., Luo Y .H., Zhang H., Gao W.P., Five inorganic–organic hybrids based on Keggin polyanion $[SiMo_{12}O_{40}]^{4-}$: From 0D to 2D network, *Journal of Solid State Chemistry,* 209 (2014) 97-104.

[21] Li S., Ma P., Niu H., Zhao J., Niu J., $\{[Cu(phen)]_3Cl_4\}_2[GeMo_{12}O_{40}]$: Synthesis, crystal structure and magnetic property of a new trinuclear copper complex based on germanomolybdate, *Inorganic Chemistry Communications,* 13 (2010) 805-808.

[22] Igarashi T., Zhang Z., Haioka T., Iseki N., Hiyoshi N., Sakaguchi N., Kato C., Nishihara S., Inoue K., Yamamoto A., Yoshida H., Tsunoji N., Ueda W., Sano T., Sadakane M., Synthesis of ε-Keggin-Type Cobaltomolybdate-Based 3D Framework Material and Characterization Using Atomic-Scale HAADF-STEM and XANES, *Inorganic Chemistry,* 56 (2017) 2042–2049.

[23] Findik M., Ucar A., Colak A.T., Sahin O., Bingol H., Sayin U., Kocak N., Self-assembly of a new building block of {BMo12O40} with excellent catalytic activity for methylene blue, *Polyhedron,* 160 (2019) 229–237.

[24] Gang Z., Bond A.M., Zhao C., Recent trends in the use of polyoxometalate-based material for efficient water oxidation, *Science China Chemistry,* 54 (2011) 1877–1887.

[25] Song Y., Tsunashima R., Recent advances on polyoxometalate-based molecular and composite materials, *Chemical Society Reviews,* 41 (2012) 7384-7402.

[26] Alamdari R.F., Zekri N., Moghadam A.J., Farsani M.R., Green oxidation of sulfides to sulfoxides and sulfones with H_2O_2 catalyzed by ionic liquid compounds based on Keplerate polyoxometalates, *Catalysis Communications,* 98 (2017) 71–75.

[27] Hasannia S., Yadollahi B., Zn–Al LDH nanostructures pillared by Fe substituted Keggin type polyoxometalate: Synthesis, characterization and catalytic effect in green oxidation of alcohols , *Polyhedron,* 99 (2015) 260–265.

[28] Sheldrick G.M., A short history of SHELX, *Acta Crystallographica Section A*, A64 (2008) 112–122.

[29] Sheldrick G.M., Crystal structure refinement with SHELXL, *Acta Crystallographica Section C;* C71 (2015) 3–8.

[30] Farrugia L.J., WinGX and ORTEP for Windows: an update, *J. Appl. Cryst.*, 45 (2012) 849–854.

[31] Wang T., Peng J., Liu H., Zhu D., Tian A., Wang L., Open framework complex constructed from polyoxometalate and dinuclear Cu–phenanthroline, *Journal of Molecular Structure*, 892 (2008) 268–271.

[32] Hu Y.Y., Zhang T.T., Zhang X., Zhao D.C., Cui X.B., Huoa Q.S., Xu J.Q., New organic–inorganic hybrid compounds constructed from polyoxometalates and transition metal mixed-organic-ligand complexes, *Dalton Transactions*, 45 (2016) 2562-2573.

[33] Chen Y., Zhou B., Zhao J., Li Y., Su Z., Zhao Z., Two novelh ybrid compounds based on $[MW_{12}O_{40}]^{5-}$ (M=B, Al) heteropolyanions and copper coordination polymer with bpp ligands, *Inorganica Chimica Acta*, 363 (2010) 3897–3903.

[34] Olgun A., Çolak A.T., Gübbük I..H., Şahin O., Kanar E., A new Keggin-type polyoxometalate catalyst for degradation of aqueous organic contaminants, *Journal of Molecular Structure*, 1134 (2017) 78-84.

[35] Chen Y., Gu X., Peng J., Shi Z., Wang E., Hydrothermal synthesis and crystal structure of organic–inorganic hybrid vanadate: $[Zn(phen)(H_2O)V_2O_6]$ (phen=1,10-phenanthroline), *Journal of Molecular Structure*, 692 (2004) 243-247.

[36] Sundararajan M.L., Jeyakumar T., Anandakumaran J., Selvan B.K., Synthesis of metal complexes involving Schiff base ligand with methylenedioxy moiety: Spectral, thermal, XRD and antimicrobial studies, *Spectrochimica Acta Part A: Molecular and Biomolecular Spectroscopy*, 131 (2014) 82–93.

[37] Iftikhar B., Javed K., Khan M.S.U., Akhter Z., Mirza B., Mckee V., Synthesis, characterization and biological assay of Salicylaldehyde Schiff base Cu(II) complexes and their precursors, *Journal of Molecular Structure*, 1155 (2018) 337-348.

[38] Wang X., Jia G., Yu Y., Gao Y., Zhang W., Wang H., Cao Z., Liu J., A New Homogeneous Electrocatalyst For Electrochemical Carbonylation Of Methanol To Dimethyl Carbonate, *Química Nova*, 38 (2015) 298-302.

[39] Küçük I., Vural S., Kıvılcım N., Adıgüzel I., Köytepe S., Seçkin T., Hydrothermal Synthesis of Polyoxometalate Containing Cobalt Ion and Its Polyurethane Composites for Dielectric Material Applications, *Polymer-Plastics Technology And Materials,* 59 (2020) 1822-1841.

[40] Ge W., Long Z., Cai X., Wang Q., Zhou Y., Xu Y., Wang J., A new polyoxometalate-based Mo/V coordinated crystalline hybrid and its catalytic activity in aerobic hydroxylation of benzene, *RSC Advance*, 4 (2014) 45816–45822.

[41] Zhang B.S., Wu C.S., Qiu J.P., Li Y.X., Liu Z.X., α-Keggin tungstogermanate-supported transition metal complexes: hydrothermal synthesis, characterization, and magnetism of $Cu_2(phen)_4(GeW_{12}O_{40})$ and $[Ni_2(bpy)_4(H_2O)_2(GeW_{12}O_{40})]_2{\cdot}H_2O$, *Journal of Coordination Chemistry*, 67 (2014) 787–796.